

# Minimum cost solution to residential energy-water nexus through rainwater harvesting and greywater recycling

Lijun Zhang <sup>a, b, \*</sup>, Ambrose Njepu <sup>b</sup>, Xiaohua Xia <sup>b</sup>

<sup>a</sup> School of Artificial Intelligence and Automation, Huazhong University of Science and Technology, Wuhan, 430074, China

<sup>b</sup> Department of Electrical, Electronic and Computer Engineering, University of Pretoria, Pretoria, 0002, South Africa



## ARTICLE INFO

### Article history:

Received 29 July 2020

Received in revised form

13 March 2021

Accepted 13 March 2021

Available online 20 March 2021

Handling editor: Prof. Jiri Jaromir Klemes

### Keywords:

Energy-water nexus

Rainwater harvesting

Greywater recycling

Sizing and operation optimization

Sensitivity analysis

Economic analysis

## ABSTRACT

This paper presents an integrated rainwater harvesting and greywater recycling system to tackle the energy-water nexus in residences with unreliable water and electricity supply. The system is made up of the municipal water and energy supplies, a rainwater harvesting system and a greywater recycling system to supply the residential water demand. A combined sizing and operational optimization approach is developed. In particular, a mixed integer linear programming model is formulated to determine the optimal sizes of the water tanks and optimal operation of pumps to reduce potable water consumption and electricity cost under the time-of-use tariff. The model formulated is applied to a practical case study of a single-family house in Durban, Kwa-Zulu Natal province of South Africa. Simulations results with measured rainfall intensity over five years show that the proposed integrated rainwater harvesting and greywater recycling system is beneficial for the household in terms of both water savings and financial cost savings with an acceptable payback period of 4.39 years. To investigate the validity of the results obtained in different applications, a sensitivity analysis was performed concerning uncertainties in water demand, rainfall intensity, the cost of electricity and discount rate. The findings confirm that the model developed is robust against uncertainties in these parameters. It is also concluded that payback period of the project can be even shorter if applied to a case with a higher water demand.

© 2021 Elsevier Ltd. All rights reserved.

## 1. Introduction

Energy and water securities are amongst the most important global challenges for sustainable development (UNDP, 2015). One-third of the world's population experiences severe water scarcity at least once in a year, while over half a billion people live under water scarcity (Vörösmarty et al., 2000). Agriculture, residential and industry are the three largest freshwater consumers globally, they account for 60%, 30% and 8% of global freshwater consumption, respectively (UNESCO, 2003). Therefore, water demand increases rapidly with population, industrial and economic growths, thus placing pressure on the limited available water resource (Letsoalo et al., 2007). The World Health Organisation (Organization, 2006) and World Bank (Jacobsen et al., 2012) reported that global water scarcity will increase by 40% in 2030 due to the unsustainable trend

of water demand and supply. The World Bank states that the degree of water scarcity will vary with regions depending on existing water infrastructures, climatic conditions, and technological advancements, thereby stating that water scarcity will increase by 43% in North America to 280% in sub-Saharan Africa by 2030 (Jacobsen et al., 2012). Similarly, energy scarcity is a global menace caused by insufficient energy to meet the rapidly growing energy demand due to population, industrial and economic growths (Huang et al., 2020), which is also well acknowledged. For instance, the United States National Intelligence Council (2013) reported that energy scarcity will increase by 50% in 2030.

The interdependence of energy and water is termed as 'energy-water nexus', which can be understood by examples of water usage in power generation and electricity use in water supply networks. One of the implications of this inter-relationship is that water scarcity will cause energy scarcity and vice versa.

In this study, the focus is on residential energy-water nexus, which refers to the inter-relationship between energy and water supply to the households. In particular, the 'nexus' in this study refers to the interplay between effective potable water and energy

\* Corresponding author. School of Artificial Intelligence and Automation, Huazhong University of Science and Technology, Wuhan, 430074, China.

E-mail address: [lijun2016@iee.org](mailto:lijun2016@iee.org) (L. Zhang).

Nomenclature			
<b>Indexes</b>			
$i, j$	Indexes of time intervals	$A_r$	Rainwater catchment area of roof [ $m^2$ ]
$m$	Index of water tanks	$R_r$	Rainwater run-off coefficient
$y$	Index of years in the project lifetime	$I_r(i)$	Rainfall intensity [mm]
<b>Superscripts</b>		$\tau$	Fraction of potable water collected for recycling
$min, max$	Minimum and maximum of a variable	$D_{t,npw}$	Volume of total non-potable water demand [ $m^3$ ]
$b$	Variable associated with the baseline case	$S_{t,npw}$	Volume of total non-potable water supply [ $m^3$ ]
<b>Symbols</b>		$J$	Daily water cost per unit volume [ $R/m^3$ ]
$N$	Total number of time intervals	$J_t$	Equivalent daily cost of water tanks [ $R$ ]
$R$	South Africa currency, rand	$J_e$	Daily electricity cost [ $R$ ]
$t_s$	Sampling interval [s]	$J_w$	Daily water cost [ $R$ ]
$A_{tm}$	Cross-sectional area of water tank $m$ [ $m^2$ ]	$J_p$	Daily pump switching cost [ $R$ ]
$H_m$	Height of water tank $m$ [m]	$D_{tot}$	Total daily water demand [ $m^3$ ]
$h_m(i)$	Water level of water tank $m$ [m]	$k_t, k_t'$	Cost of rooftop and underground water tanks per unit volume [ $R/m^3$ ]
$Q_1, Q_2$	Water flow rate of pumps 1 and 2 [ $m^3/s$ ]	$A_F$	Annuity factor used to calculate equivalent annual cost of water tanks
$Q_3$	Water flow rate of the unidirectional valve [ $m^3/s$ ]	$r$	Discounting factor
$D_{pw}(i)$	potable water demand [ $m^3/s$ ]	$L$	Project lifespan
$D_{npw}(i)$	Non-potable water demand [ $m^3/s$ ]	$\rho_e(i)$	Time-of-use electricity cost [ $R/kWh$ ]
$u_1(i), u_2(i)$	Binary variables indicating the on/off status of pumps 1 and 2, equal to one when the pump is on	$\rho_{pw}$	Potable water cost [ $R/m^3$ ]
$u_3(i)$	Binary variable indicating the on/off status of the unidirectional valve, equal to one when the valve is open	$\rho_{npw}$	Non-potable water cost [ $R/m^3$ ]
$V_{gw}(i)$	Volume of collected greywater [ $m^3$ ]	$\rho_s$	Cost of a single pump switch [ $R/switch$ ]
$V_{rw}(i)$	Volume of collected rainwater [ $m^3$ ]	$s_1, s_2$	Auxiliary binary variables used to determine the numbers of pump switching
$V_{ov}(i)$	Volume of underground water tank overflow [ $m^3$ ]	$X$	Decision vector
		$f$	Coefficient vector of cost function
		$M, b$	Matrix and vector of inequality constraints
		$M_{eq}, b_{eq}$	Matrix and vector of equality constraints
		$L_b, U_b$	Lower and upper bounds of decision vector
		$CF(y)$	Cash flow in year $y$ [ $R$ ]

utilisation in a residential home in terms of reducing potable water and energy used to meet the household's water demand, and reducing the electrical grid's pressure on electricity supply. To address the conservation of water and energy resources, existing studies have examined groundwater extraction (Gleeson et al., 2010), seawater desalination (Pinto and Marques, 2017), rainwater harvesting (RWH) (Boers and Ben-Asher, 1982) and greywater recycling (GWR) (Li et al., 2009) for residential applications (Ghisi and de Oliveira, 2007). Concludes that RWH and GWR systems are the most sustainable solutions to water scarcity in residences. Further, a recent study confirmed that single-family houses have the highest potential of energy savings using a combination of toilets replacement, greywater reuse, and rainwater harvesting in the city of Joinville (Cureau and Ghisi, 2020). Therefore, this study proposes an integrated RWH-GWR system as an environmentally and economically sustainable demand side solution to the challenges of energy-water nexus in residences. The RWH and GWR systems are briefly introduced in the subsequent paragraphs for the completeness of this paper.

Rainwater harvesting involves the collection, treatment, storage and use of rainwater for domestic, industrial and agricultural purposes. It is gaining renewed interest and attention due to the widespread water scarcity. There are two types of RWH system namely, the rooftop and run-off RWH systems. The rooftop RWH system collects water from a rooftop catchment area, while the run-off RWH system traps and collects contaminated run-off or stormwater for use (Imteaz et al., 2011). The rooftop RWH is economical and most suitable for residences, therefore it is used in this study and any mention of the RWH system subsequently refers to the rooftop RWH system. The quality of harvested rainwater

depends on the atmospheric impurity level, catchment area, water treatment, storage, and distribution pipes (Sanchez et al., 2015). However, the use of rainwater for non-potable purposes require at most primary treatment, while first-flush and filtration are the least recommended treatments for potable end-uses (Gwenzi et al., 2015). The performance of a RWH system, in terms of potable water savings and reliability, varies with rainfall parameters (Ghisi and de Oliveira, 2007) and catchment area (Farreny et al., 2011). It performs best in wet regions (wet years in dry regions) with a large catchment area and high non-potable water utilisation rate. In terms of economical performance, RWH systems have a payback period between 2 – 35 years depending on the application. For instance (Ghisi and Schondermark, 2013), studied a large number of different residential buildings (Domènech and Saurí, 2011), studied a large multi-family building, and (Chilton et al., 2000) studied a commercial building.

Greywater is wastewater without fecal contamination that is collected from the kitchen sinks, showers or baths, and laundry machines. The GWR system is an assembly that collects, treats and stores greywater for re-use (Ilemobade et al., 2013). Greywater supply is reliable and it accounts for 43 – 70% of the total wastewater generated in residences (Siang et al., 2018). (Prathapar et al., 2005) report that GWR has the potential of reducing 30 – 50% potable water usage for irrigation and toilet flushing. Water treatment is essential to maximize the performance of GWR systems. Greywater treatment is classified into three stages namely, physical, biological and chemical treatments (Boyjoo et al., 2013). The physical treatment removes solids, organics and surfactants. The biological treatment eliminates pathogen, while chemical treatment disinfects the water for safe use (Ghunmi et al., 2011). Some

common biological water treatment methods include rotary biological contactors (RBC) (Li et al., 2009), biological aerated filters (BAF) (Al-Jayyousi, 2003) and membrane bio-reactors (MBR) (Jeong et al., 2018). Common chemical disinfectants include hypochlorite, chlorine, ozone, and ultraviolet radiation. Generally, GWR is an energy and capital intensive process that is mainly due to the energy and capital intensive nature of the water treatment process (Christova-Boal et al., 1996). Therefore (Siang et al., 2018), proposed a fit-for-purpose water treatment that delivers tailored treatment depending on end-use points and the required water quality.

There are two variants of the RWH-GWR system reported in the literature, namely, independent RWH-GWR systems and integrated RWH-GWR systems. In the independent RWH-GWR systems, the RWH and GWR subsystems are completely isolated from each other, while the RWH and GWR subsystems in the integrated RWH-GWR subsystems share water treatment and storage facilities. It is also revealed that the performance of the RWH and GWR subsystems affect the performance of the overall system (Kim et al., 2007). All three systems (RWH, GWR and RWH-GWR systems) have high water savings potential and long payback periods, however, their relative performance varies with rainfall, occupancy rate, and non-potable water utilisation (Ghisi and de Oliveira, 2007). Researchers agree that GWR systems are more effective in densely populated locations, multi-story and multi-family buildings, RWH subsystems are more effective in locations with regular rainfall, and the integrated RWH-GWR system is the most effective, reliable and robust alternative irrespective of population density and rainfall properties according to (Zhang et al., 2009) and (Leong et al., 2018).

This paper investigates the benefits of integrated RWH-GWR systems when implemented in residential areas in South Africa, a semi-arid country possessing an average annual rainfall of 500 mm. Motivations for this are twofold. On the one hand, South Africa is facing severe water and energy insecurities similar to many countries in the world. With prolonged droughts, the City of Cape Town and City of Johannesburg had been implementing water restrictions in the past few years. Additionally, the country's national utility grid is struggling to supply its customers and a lot of electricity load shedding had been and are still being put into place, leaving its people with unreliable water and energy supplies. On the other hand, residential areas of South Africa are characterized by scattered settlements in the form of communities or individual houses. Each household usually owns a garden that requires regular irrigation, placing more demand for water. Therefore, an integrated RWH-GWR system is proposed to improve water security through water recycling and harvesting and to improve energy security and reduce electricity cost by shifting electricity demand out of peak demand periods taking advantage of the water storage tanks in the RWH-GWR system for residential households.

For this purpose, the design and operation of the RWH-GWR system are essential to ensure its efficient operation and maximize its benefits. From the design perspective, the sizing of the water tanks required by the system plays an important role in both the water saving and cost implications of the RWH-GWR system. There are direct relationships between tank sizing, water savings potential (Ghisi et al., 2007) and the reliability of water supply systems (Notaro et al., 2016), and an inverse relationship between tank sizing and the economic attractiveness of the water supply systems (Ghisi and Schondermark, 2013) because increased capital investment on large tanks will improve the water savings potential and the reliability of water supply systems at the expense of its economic attractiveness. Furthermore, tank sizing is affected by internal and external factors such as demand profile, rainfall, weather, and climatic conditions, thereby increasing the complexities of accurate tank sizing. The size of the water tanks thus

should be determined optimally such that it meets the required water storage for the operation of the system and reduces the project's capital cost.

Studies on tank sizing include: the water balance model (Thapa et al., 2017), probabilistic method (Su et al., 2009), reliability curve method such as (Karim et al., 2013) and (Khastagir and Jayasuriya, 2010), minimum cost based and regressive model approach (Campisano and Modica, 2012), linear programming method (Okoye et al., 2015), mass diagram method (Komeh et al., 2017) and Neptune computer programming method (Ghisi and Ferreira, 2007). (Matos et al., 2013) states that the Rippl method and the daily simulation method using the 80 % efficiency criteria are the most cost-effective tank sizing methods because of their high economic savings to installation cost ratio. These studies are mainly about the RWH system or generic tank sizing in water systems, while GWR systems assume fixed tank size to meet the daily water demand only. For the integrated RWH-GWR system, studies have focused on its tank sizing, potable water savings potential estimation and economic attractiveness. For example (Ghisi and de Oliveira, 2007), and (Ghisi and Ferreira, 2007) studied the water savings potential estimation of RWH-GWR systems when applied to Southern Brazil and concluded that system, although it can result in about 33.8–36.4% and 39.2–42.7% potable water savings in single and multi-story buildings, is not economically viable because of its long payback period (PBP). Aligning with this conclusion (Zhang et al., 2009), investigated a distributed water treatment system for RWH-GWR systems to improve the economic benefits of such systems. However, the operational aspects were not taken into account in the design studies.

From an operational point of view, an open-loop optimal control and a closed-loop model predictive control strategies for an integrated RWH-GWR system were developed and their relative performances were compared without considering tank sizing (Wanjiru and Xia, 2018). Other studies on operational optimization of multiple pumps such as (Zhuang and Xia, 2013) published also do not take into account the sizing of the water tanks/reservoirs.

As such, the studies reported investigated either the design or operation of RWH-GWR systems. The interplay between water tank sizing and pump operation optimization is not exploited. In practice, these two are highly dependent. For instance, a big tank contributes to reducing the electricity cost by shifting pump operations out of peak demand period whereas a small tank contributes to less investment. A holistic approach that takes both water tank sizing and pumps operation optimization into account is thus much needed to improve the overall performance of RWH-GWR systems.

To address this need, this paper introduces the first attempt to develop a model for optimal tank sizing and operation of the integrated RWH-GWR system for residential applications under the time-of-use (TOU) electricity tariff. The objective is to, firstly, reduce the potable water consumption of the household to improve water security by combing the benefits of RWH and GWR systems; and secondly, improve the economic attractiveness of integrated RWH-GWR system by minimising capital cost on water tanks and operational cost, simultaneously. This also contributes to addressing the energy security challenge by reducing grid strain in peak demand periods. In short, this work contributes to the body of knowledge by developing a combined water tank sizing and pump operation optimization model for RWH-GWR systems to tackle the challenges of water and energy security that at the same time improves the system's economic attractiveness. Furthermore, sensitivity analysis is conducted to evaluate the robustness of the proposed model against uncertainties including rainfall intensity, water demand, electricity price, and discount rate. Some insights into this analysis are also provided to guide applications of the RWH-GWR systems.

This paper is organized as follows: Section 2 shows the mathematical model of the proposed RWH-GWR system. Section 3 shows the optimization model, Section 4 provides information about the case study. Section 5 contains the simulation results, discussion, Pareto, economic and sensitivity analyses of the proposed model and finally, Section 6 gives the conclusion.

## 2. Mathematical model formulation

This section provide detailed mathematical formulation of the residential minimum cost water supply problem using an RWH-GWR system.

### 2.1. Schematic model layout

Fig. 1 shows the schematic layout of the proposed residential water supply system. It is made-up of the RWH system, GWR system, storage system, pumps and municipal energy and water supplies. In this study, the connected RWH-GWR subsystems are adopted. Therefore, the RWH and GWR subsystems share the water treatments, water tanks, non-potable water pump, and end-use points. In addition to the rooftop catchment area and the grey-water collection points for the RWH and GWR systems, respectively. The storage system comprises of the rooftop potable ( $T_1$ ) and non-potable water ( $T_2$ ) tanks, and the underground tank ( $T_3$ ). The rooftop potable water tank collects water that is pumped from the municipal line to the rooftop potable water tank. Similarly, the rooftop non-potable water tank receives treated non-potable water (rain and greywater mixture) that is pumped from the underground tank by the non-potable water pump. The municipal potable water supply is used to meet the residential potable water demand, while the non-potable water supply is used to meet the residential non-potable water demand that includes toilet flushing and irrigation. In cases when the non-potable water tanks ( $T_2$  and  $T_3$ ) are unable to meet their demand, potable water is released from the rooftop potable water tank through a unidirectional valve to meet this demand.

The mathematical model of the subsystems is given in the following.

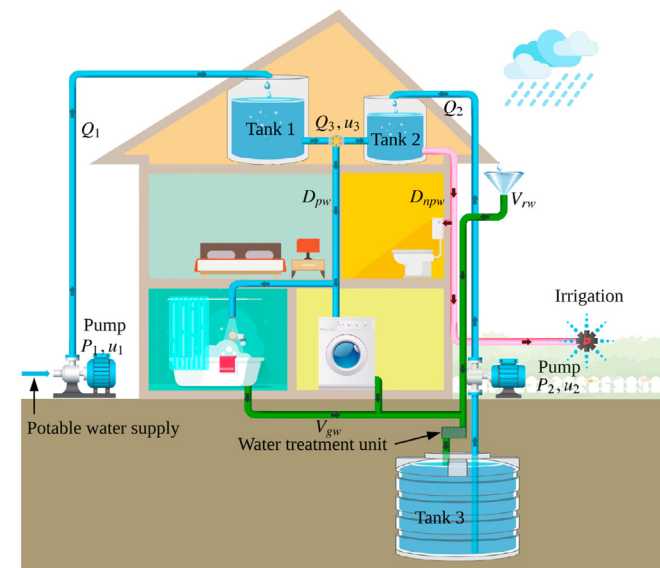


Fig. 1. Schematic layout the proposed residential RWH-GWR system.

### 2.2. Water storage tanks

All three water tanks are cylindrical, uniform cross-sectional area tanks that collect, hold and release water to meet the residential demands. The water levels in the tanks at time intervals  $j = 1, 2, \dots, N$  are expressed as:

$$h_1(j) = h_1(0) + \frac{1}{A_{t1}} \sum_{i=0}^{j-1} [t_s Q_1 u_1(i) - t_s Q_3 u_3(i) - D_{pw}(i)], \quad (1)$$

$$h_2(j) = h_2(0) + \frac{1}{A_{t2}} \sum_{i=0}^{j-1} [t_s Q_2 u_2(i) + t_s Q_3 u_3(i) - D_{npw}(i)], \quad (2)$$

$$h_3(j) = h_3(0) + \frac{1}{A_{t3}} \sum_{i=0}^{j-1} [V_{gw}(i) + V_{rw}(i) - t_s Q_2 u_2(i) - V_{ov}(i)]. \quad (3)$$

The volume of rainwater collected by the RWH system is expressed as (Ghisi and de Oliveira, 2007; Farreny et al., 2011):

$$V_{rw}(i) = \frac{A_r R_c I_r(i)}{1000}. \quad (4)$$

The volume of greywater collected is defined as a fraction of the potable water demand as (Wanjiru and Xia, 2018):

$$V_{gw}(i) = \tau D_{pw}(i). \quad (5)$$

The harvested rain and greywater collected are treated and stored in the underground tank for later use. Water is lost to tank overflow when the volume of the non-potable water in the tank exceeds the size of the tank (Notaro et al., 2016):

$$V_{ov}(i) = \begin{cases} A_{t3} (h_3(i) - h_3^{max}), & \text{if } h_3(i) > h_3^{max}, \\ 0, & \text{otherwise.} \end{cases} \quad (6)$$

## 3. Optimization model

A mixed binary linear programming problem is formulated to solve the problem stated in the preceding sections. The objective is to minimize the daily cost of the water supply system:

$$J = \frac{J_t + J_e + J_w + J_p}{D_{tot}}, \quad (7)$$

where  $D_{tot} = \sum_{j=1}^N (D_{pw}(j) + D_{npw}(j))$  is the total water demand.  $J_t$  is the equivalent daily cost of water tanks:

$$J_t = \frac{k_t (A_{t1} H_1 + A_{t2} H_2) + k_t' A_{t3} H_3}{365 A_F}, \quad (8)$$

where  $k_t' > k_t$  in general and the annuity factor

$$A_F = \frac{1 - 1/(1+r)^L}{r} \quad (9)$$

converts the tanks' capital and maintenance costs into equivalent annual costs taking into account time value of money (Sasmitha, 2010).  $J_e$  is the daily electricity cost:



$$J_e = t_s \sum_{j=1}^N \rho_e(j) [P_1 u_1(j) + P_2 u_2(j)]. \quad (10)$$

$J_w$  is the daily water cost:

$$J_w = t_s \sum_{j=1}^N [\rho_{pw} Q_1 u_1(j) + \rho_{npw} Q_2 u_2(j)]. \quad (11)$$

And,  $J_p$  is introduced to minimize the switching frequency of the pumps in order to alleviate pump aging as pointed out in (Lansey and Awumah, 1994; Menke et al., 2016) etc. following the method developed in (Mathaba et al., 2014) by adopting the cost function:

$$J_p = \rho_s \sum_{j=1}^N [s_1(j) + s_2(j)]. \quad (12)$$

The optimization problem is subject to the following constraints:

$$u_m \in \{0, 1\}, \text{ for } m = 1, 2, 3. \quad (13)$$

$$s_1, s_2 \in \{0, 1\}, \quad (14)$$

$$u_1(j) - s_1(j) \leq 0, \quad (15)$$

$$u_1(j) - u_1(j-1) - s_1(j) \leq 0, \quad (16)$$

$$u_2(j) - s_2(j) \leq 0, \quad (17)$$

$$u_2(j) - u_2(j-1) - s_2(j) \leq 0, \quad (18)$$

$$h_1^{min} \leq h_1(j) \leq H_1, \text{ for } j = 1, 2, \dots, N, \quad (19)$$

$$h_2^{min} \leq h_2(j) \leq H_2, \text{ for } j = 1, 2, \dots, N, \quad (20)$$

$$h_3^{min} \leq h_3(j) \leq H_3, \text{ for } j = 1, 2, \dots, N, \quad (21)$$

$$H_1^{min} \leq H_1 \leq H_1^{max}, \quad (22)$$

$$H_2^{min} \leq H_2 \leq H_2^{max}, \quad (23)$$

$$H_3^{min} \leq H_3 \leq H_3^{max}. \quad (24)$$

Constraints (13)–(14) are boundary constraints for the binary decision variables. Constraints (15)–(17) initialise the auxiliary variables as the initial status of the pump switches. Constraints (16)–(18) minimize the switching frequency of the pumps by augmenting adjacent switchings. Constraints (19)–(21) are respectively, the boundary constraints on the water level ( $h$ ) in the potable water, non-potable water and underground tanks. The dynamics of the water levels are controlled by the switching of the decision variables in Equations (1)–(3). Constraints (22)–(24) are the boundary constraints for the storage volume of the potable water, non-potable water and underground tanks, respectively.

The mathematical model formulated can be expressed in standard linear form as:

$$\min f^T X, \quad (25)$$

subject to

$$\begin{cases} MX \leq b; & \text{linear inequality constraint,} \\ M_{eq}X = b_{eq}; & \text{linear equality constraint,} \\ L_b \leq X \leq U_b; & \text{boundary constraint,} \end{cases} \quad (26)$$

Therefore, the optimization model can be expressed as:

$$f = \frac{1}{D_{tot}} \left[ \frac{k_t A_{t1}}{365 A_F}, \frac{k_t A_{t2}}{365 A_F}, \frac{k_t A_{t3}}{365 A_F}, t_s (P_1 \rho_e(1) + \rho_{pw} Q_1) \dots t_s (P_1 \rho_e(N) + \rho_{pw} Q_1), t_s (P_2 \rho_e(1) + \rho_{npw} Q_2) \dots t_s (P_2 \rho_e(N) + \rho_{npw} Q_2), \mathbf{0}_{1 \times N}, \rho_s \mathbf{1}_{1 \times 2N} \right]^T_{(3+5N) \times 1}, \quad (27)$$

$$X = [H_1, H_2, H_3, u_1(1) \dots u_1(N), u_2(1) \dots u_2(N), u_3(1) \dots u_3(N), s_1(1) \dots s_1(N), s_2(1) \dots s_2(N)]^T_{(3+5N) \times 1}, \quad (28)$$

The matrices and vectors of the inequality constraints can be found in the appendix. These are combined and expressed in the form of  $MX \leq b$  with:

$$M = \begin{bmatrix} M_1 \\ M_2 \\ M_3 \\ M_4 \\ M_5 \\ M_6 \\ M_7 \end{bmatrix}_{7N \times (3+5N)}, \quad b = \begin{bmatrix} b_1 \\ b_2 \\ b_3 \\ b_4 \\ b_5 \\ b_6 \\ b_7 \end{bmatrix}_{7N \times 1}, \quad (29)$$

There are no equality constraints, hence its matrix and vector are empty. Finally, the vectors of the boundary constraints are

$$L_b = [H_1^{min} \quad H_2^{min} \quad H_3^{min} \quad 0 \quad \dots \quad 0]_{(3+5N) \times 1}^T, \quad (30)$$

$$U_b = [H_1^{max} \quad H_2^{max} \quad H_3^{max} \quad 1 \quad \dots \quad 1]_{(3+5N) \times 1}^T, \quad (31)$$

These matrices and vectors are given in the Appendix.

Remark 1. Energy water nexus: the energy water ‘nexus’ mentioned in the introduction refers to the interplay between energy and water utilisation in residential houses. To this regards, the optimization problem provides a solution to this nexus by means of minimising the cost of water supply. This is equivalent to minimising water utilisation and electricity supply pressure of the electrical grid while still satisfying the household’s water demand. In case ones wants more flexibility in fine tuning the trade off between water and energy utilisation, the following modified objective function can be used:

$$J' = \frac{J_t + w_e J_e + J_w + J_p}{D_{tot}} \quad (32)$$

where  $w_e$  can be used as a weighting factor to adjust the optimization result. A larger  $w_e$  can be imposed to further reduce the electricity usage.

#### 4. Case study

A single-family building in Durban, KwaZulu-Natal province of South Africa is selected as the case study for this research. The building is occupied by a middle-class family with indoor and outdoor water end-use points. The residential water demand is satisfied by the municipal water supply, which is pumped onto the rooftop tank from where the water is released under gravity to

meet all the residential demand to cope with water and electricity supply outages. The pump involved is operated manually following a simple logic that switches on the pump when the tank is empty and switches the pump off when the tank is full. In order to determine the benefits of the proposed RWH-GWR system, a fair comparison between the existing system and the RWH-GWR system is essential. Such a fair comparison is the key to avoid over-estimation of the proposed RWH-GWR system. To this end, one has two options. One is to compare the cost of the RWH-GWR system against the manually operated existing system. One could argue, however, that this option ignored the potential cost reduction of the existing system by simply introducing an optimal operating strategy for the pump, which costs much less than the RWH-GWR system. To avoid this doubt, the second option is to compare the water supply cost of the RWH-GWR system against an improved version of the existing system, in which the pump is operated optimally. Therefore, an optimal pump operation optimization model is formulated here to minimize the electricity cost of the existing system subject to TOU tariff as follows.

$$\min J^b = \sum_{j=1}^N t_s \rho_e(j) P_1 u_1^b(j),$$

$$\text{s.t. } h_1^{\min} \leq h_1^b(0) + \frac{1}{A_{t1}} \sum_{i=0}^{j-1} [t_s Q_1 u_1^b(i) - D_{tot}(i)] \leq h_1^{\max} \quad (33)$$

$$u_1^b \in \{0, 1\}.$$

The existing water tank is a cylindrical one with a cross-sectional area of 0.5 m<sup>2</sup>, and minimum and maximum water level bounds of 0.1 m and 1.0 m, respectively. The pump is rated at 700 W with a flow rate of 0.55 m<sup>3</sup>/h. Fig. 2 shows the water demand profile of the residence. The results obtained by this optimization model using this information are shown in Fig. 3 and are used as the baseline to evaluate the benefits of the proposed RWH-GWR systems. In Fig. 3 and the figures that follow, light red, light yellow, and light green background colours are used to indicate peak, standard, and off-peak demand periods, respectively.

The proposed RWH-GWR system is limited with a rainwater catchment area of 100 m<sup>2</sup>. The GWR system collects water from the collection points for treatment, storage and redistribution to end-use points. Two additional non-potable water tanks (i.e. the rooftop non-potable water and underground tanks) are introduced to improve non-potable water utilisation and the reliability of the water supply system. The potable and non-potable water pumps are the same, with rated power at 700 W and flow rate of 0.55 m<sup>3</sup>/h. Table 1 shows the physical parameters of the potable water, non-potable water and underground tanks in the proposed system.

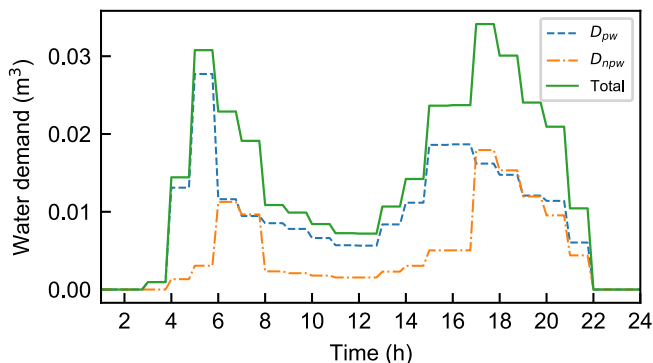


Fig. 2. Residential water demand profile.

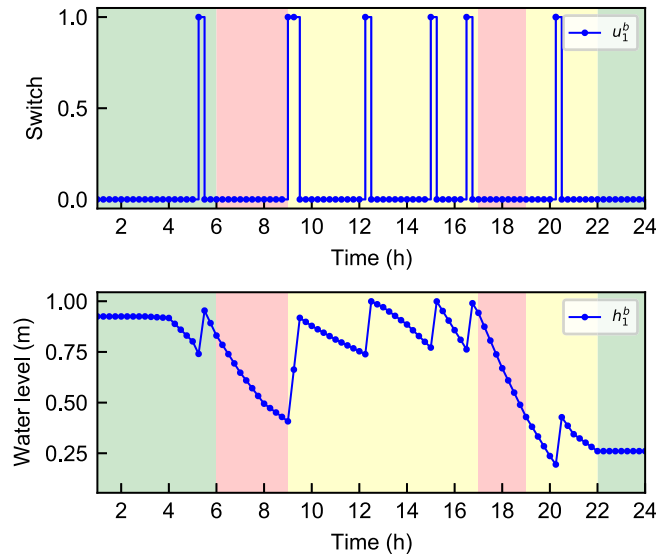


Fig. 3. Baseline pump switching and water level.

Table 1 Physical parameters of the water tanks.

Water tanks	Area (m <sup>2</sup> )	H <sup>min</sup> (m)	h <sub>i</sub> (0) (m)	H <sup>max</sup> (m)
T <sub>1</sub>	1.36	0.1	0.15	1.0
T <sub>2</sub>	1.0	0.1	0.15	1.0
T <sub>3</sub>	1.0	0	0	1.5

Table 2 Potable water and waste water discharge tariffs.

Volume (m <sup>3</sup> )	0–6	7–25	26–30	31–45	≥ 45
Potable water rates (R/m <sup>3</sup> )	0	17.23	23.59	51.99	57.18
Discharge rates (R/m <sup>3</sup> )	0	6.01	8.25	18.14	19.99

Regarding rainfall intensity, historical data from the Durban weather station in KwaZulu-Natal province shown in Fig. 5 is used.

#### 4.1. Water tariffs

Table 2 shows the incremental block water tariff structure for domestic customers in the city of Durban.<sup>1</sup> Unlike the TOU electricity tariff that the cost of electricity increases with the time of the day, the cost of water increases with the volume of water consumed in the incremental block tariff. The cost of water is lowest at the first block of water consumption and increases with the range of water consumed. In this study, the water tariff contains the incremental block tariffs for potable water consumption and wastewater discharged to the treatment plant provider by the eThekweni municipality.<sup>2</sup>

The greywater treatment cost is 4 R/m<sup>3</sup> using the DeHoust GWM products, which use BioMembrane technology to produce clear, odourless and germ-free water quality conforming to the British Standard 8525-:2010 for greywater reuse systems, EU bathing water directive 2006/7/EC, and DIN 19650 class 2.<sup>3</sup>

<sup>1</sup> [http://www.durban.gov.za/Resource\\_Centre/Services\\_Tariffs/Water%20Tariffs/Forms/AllItems.aspx](http://www.durban.gov.za/Resource_Centre/Services_Tariffs/Water%20Tariffs/Forms/AllItems.aspx).

<sup>2</sup> [http://www.durban.gov.za/Resource\\_Centre/Services\\_Tariffs/Water%20Tariffs/Forms/AllItems.aspx](http://www.durban.gov.za/Resource_Centre/Services_Tariffs/Water%20Tariffs/Forms/AllItems.aspx).

<sup>3</sup> <https://akwasolv.co.za/products/>, [https://www.akwasolv.co.za/wp-content/uploads/2018/06/WG68\\_GWM\\_500\\_datasheet.pdf](https://www.akwasolv.co.za/wp-content/uploads/2018/06/WG68_GWM_500_datasheet.pdf).

## 4.2. Electricity tariff

The TOU electricity tariff is a pricing structure that varies the cost of electricity with the time of the day, day of the week and season of the year to encourage demand response practices.

Eskom, the South African utility company, introduced the Miniflex TOU tariff structure for residential customers. The local authority Miniflex structure divides a day into peak, standard, and off-peak demand periods and is given as<sup>4</sup>:

$$\rho_e(t) = \begin{cases} 0.5732, & \text{if } t \in [0, 6] \cup [22, 24] : \text{off - peak,} \\ 1.0504, & \text{if } t \in [9, 17] \cup [19, 22] : \text{standard,} \\ 3.4520, & \text{if } t \in [6, 9] \cup [17, 19] : \text{peak.} \end{cases} \quad (34)$$

where  $t$  is the time of the day.

## 5. Simulation results and discussion

In simulations, the sampling interval is set to  $t_s = 15$  minutes. Optimal tank sizing and pump scheduling using the case study in Section 4 are investigated. It noted that the model developed deals with two time scales. Firstly, the operation of the pumps and valve need to be optimized over 24 h. Secondly, sizes of the water tanks must be optimized on yearly basis to take into account seasonal changes in the rainfall intensity. Further, the yearly variations on rainfall intensity could also have an impact on the tank sizing as indicated by (Soares Geraldi and Ghisi, 2018).

In order to size the tanks taking into account of seasonal and multiple year rainfall variations, hourly averaged rainfall data was measured at a weather station close to the studied household over five years from 01 December 2015 to 30 November 2020. South Africa has a wet southern hemisphere's summer between October and March, and a dry winter and spring from April to September. Fig. 5 shows the highest and lowest rainfall intensities over a day in the dry and wet seasons, respectively. Fig. 4 presents the detailed procedure followed to make use of the 5-year measured rainfall data. In short, the tank sizes and operation optimization of pumps are determined using the 5-year averaged rainfall data and the resulting sizing and pump schedules are simulated using the actual measured rainfall intensity over the 5-year period. The discounted payback periods obtained by the 5-year average data (DPP\_average) is compared to that determined using simulation with actual rainfall data (DPP\_actual) to evaluate the impacts of multi-year rainfall variation.

### 5.1. Optimal operation of the proposed RWH-GWR system

Simulation results of the developed sizing and operational optimization model of the RWH-GRW system are briefly summarized in this section.

Since quantitative analysis on pump maintenance cost with respect to number of pump switching is very scarce, the pump switching penalty cost  $\rho_s$  is some times determined by trail and error method that minimizes the number of switching while the operational constraints of the water supply system are honoured, such as (van Zyl et al., 2004). In view of this,  $\rho_s$  can be viewed as a tuning parameter according to the pumps involved. When  $\rho_s = 1$ , the sizes of the rooftop potable water tank, rooftop non-potable water tank and underground tank determined by the optimization model are, 544 L, 250 L and 174 L, respectively. In this case, Fig. 6 shows the operational aspects of the results for the day 01 Jan

2020. It can be seen that the model operates the pumps out of the peak demand periods to minimize electricity costs in meeting the water demand.

To demonstrate that the model is able to provide decision-makers the flexibility to fine-tune the results based on different preferences over capital cost, operating cost and pump switching cost, one more set of results with  $\rho_s = 0$  is presented in Fig. 7. It can be seen that the model operates the pumps out of the peak demand periods to minimize electricity costs in meeting the water demand. The number of pump switches is increased to ten in Fig. 7 from seven in Fig. 6.

In this case, the rooftop non-potable water tank size is increased to 252 L and the underground water tank size is reduced to 137 L because the pump switching cost is not considered. This illustrates that decision-makers can tune the weighting factors to obtain the results that work the best for their pumps.

### 5.2. Economic analysis

It is important to evaluate the economic feasibility of any project. There are a number of different economic indicators such as internal rate of return, life cycle costs, etc. that can be used for this purpose (Sasmitha, 2010). They however all serve the purpose of giving the decision maker an indication of the profitability of the project. To this end, they are equivalent and have their own pros and cons. For instance, both discounted payback period (DPP) and life cycle cost all takes into account the time value of money. The latter, however does not consider the economic savings achieved from the project. Internal rate of return, on the other hand, determines the discounting rate that makes the project's net present value equals to zero. The DPP is very intuitive in the sense that it give a clear idea about the time required for the investment to repay itself and is used extensively by decision makers. Therefore, DPP is used in this study to evaluate the economic feasibility of the proposed system and is calculated by:

$$DPP = m_y + \frac{Y}{Z} \quad (35)$$

where  $m_y$  is the last year with negative accumulative discounted cash flow (ADC). In other words,  $m_y$  is the largest number that makes

$$ADC = \sum_{y=0}^{m_y} \frac{CF(y)}{(1+r)^i} \quad (36)$$

negative, where  $r$  is the discounting factor and  $CF_i$  is the net cash flow in the  $i$ -th year.  $Y$  is the absolute value of  $ADC$  and  $Z$  is the discounted cash flow in the next year,  $CF_{m_y+1}$ . In this study, the capital cost includes the purchasing and installation cost of water tanks, pumps, water treatment and other accessories, which are determined from the local suppliers and consultants and shown in Table 3.

The figures given in Table 3, together with the operation optimization result, are used to determine the net annual operating and maintenance cost savings of the RWH-GWR system shown in Table 4. In the DPP calculation, the maintenance cost is taken as 10% of the capital cost of the pumps, tanks, and water treatment systems, a constant discount rate of 5.2% is assumed, which is the inflation rate of South Africa in 2018. By contrast, the cost of electricity increases by 15% in the first three years of the project and reduces to 9.6% in the fourth year and assumed to remain constant for the remainder of the project according to South Africa's electricity price increase plan. Potable water tariff increases 15% and the

<sup>4</sup> [https://www.eskom.co.za/CustomerCare/TariffsAndCharges/Documents/Eskom%20schedule%20of%20standard%20prices%202018\\_19.pdf](https://www.eskom.co.za/CustomerCare/TariffsAndCharges/Documents/Eskom%20schedule%20of%20standard%20prices%202018_19.pdf).

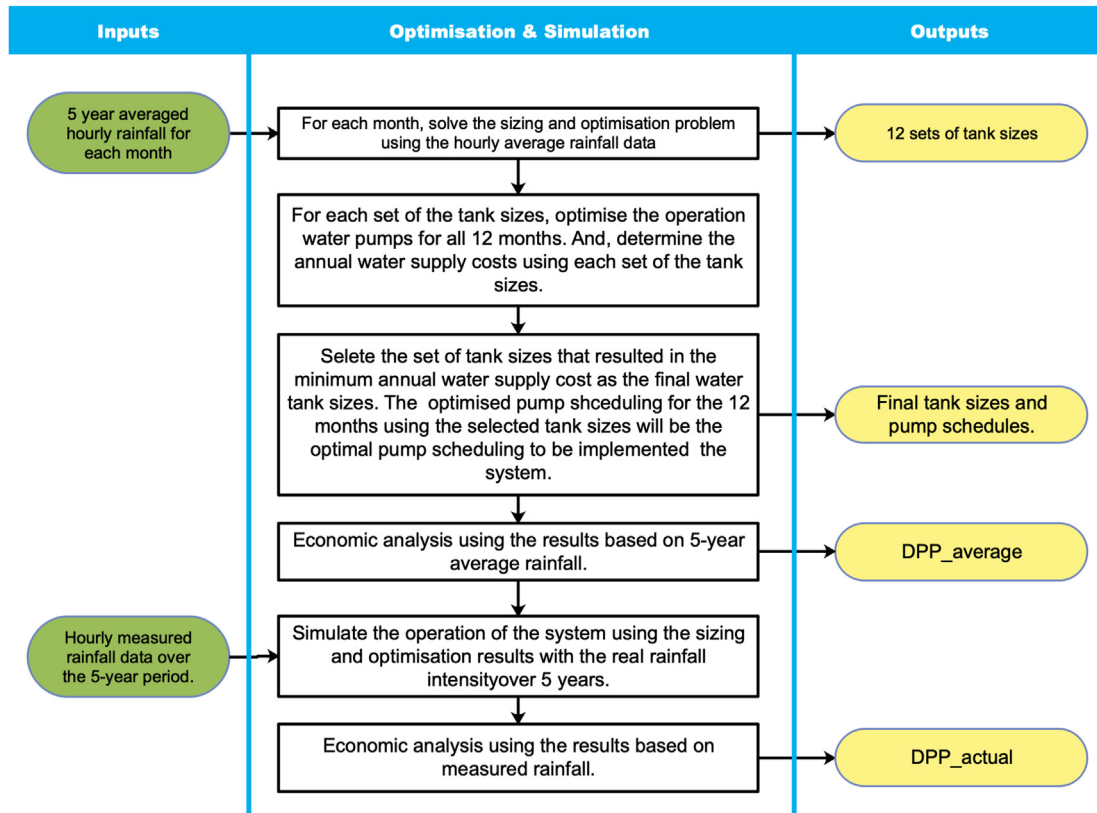


Fig. 4. Workflow of the optimal tank sizing and operational optimization.

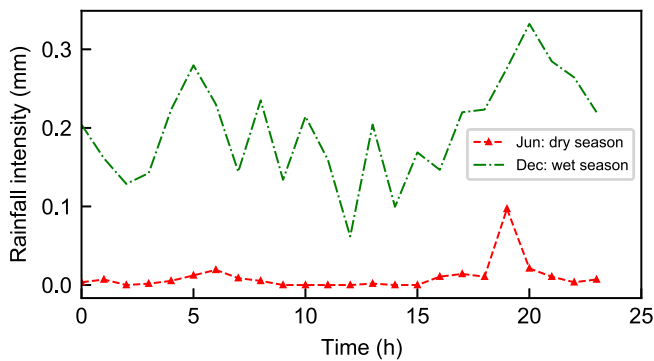


Fig. 5. Measured hourly average rainfall intensity in Durban, South Africa.

wastewater disposal tariff increases 9.9% every year according to the Municipality’s historical price increase trend. And the service life of the project is  $L = 15$  years.

Using the above information and following (39), the DPP (corresponding to DPP\_average in Fig. 4) of the project was determined as 4.39 years. Detailed economic analysis data is shown in Table 5. This demonstrates the benefits of the model presented in this study in comparison to the results obtained by (Ghisi and de Oliveira, 2007) and (Wanjiru and Xia, 2018), which indicated that the integrated RWH-GWR system does not repay its investment in its lifetime.

In addition, the DPP was also determined by simulating the system’s operation over the 5 years using actual hourly measured rainfall data in order to verify that the economic analysis result based on the 5-year average rainfall data can accurately reflect the reality. This DPP (corresponding to DPP\_actual in Fig. 4) is

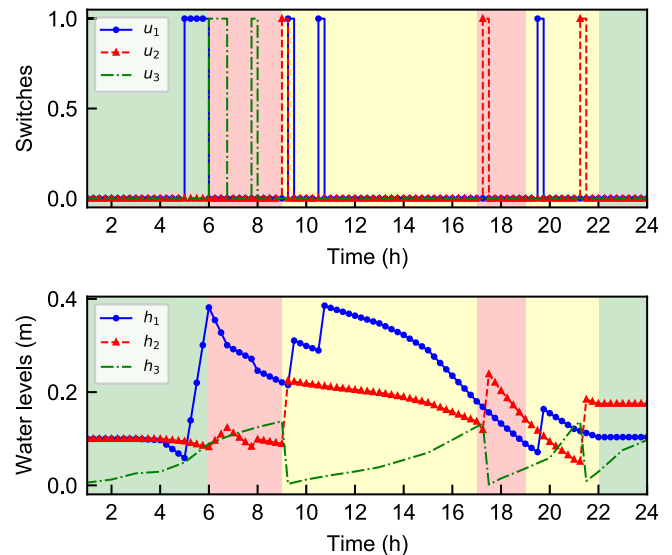


Fig. 6. Operation of the proposed system on 2020-01-01 with  $\rho_s = 1$

determined to be 4.65 years, which is 5.9% higher than that determined using the 5-year average rainfall data. This demonstrates that the economic performance of the proposed system can be reasonably estimated using averaged rainfall data over 5 years which acceptable accuracy, which is in line with conclusion drawn by (Soares Geraldini and Ghisi, 2018): “the use of short-term time series instead of 30-year time series for the simulation of rainwater harvesting systems is valid, depending on the rainfall characteristics of the region”.



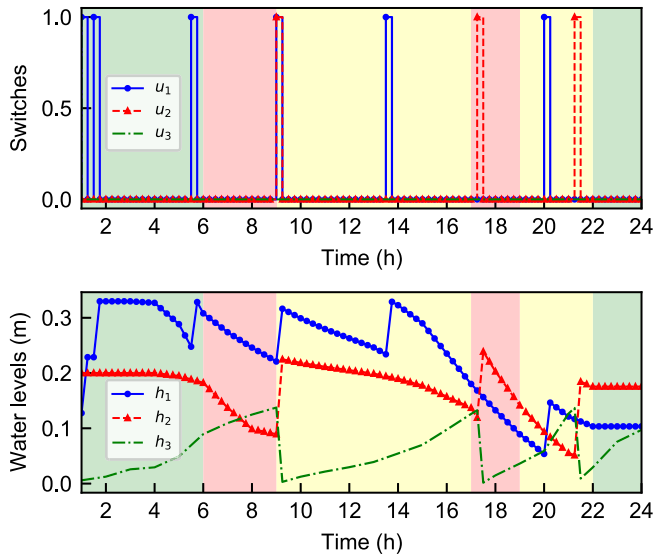


Fig. 7. Operation of the proposed system on 2020-01-01 with  $\rho_s = 0$

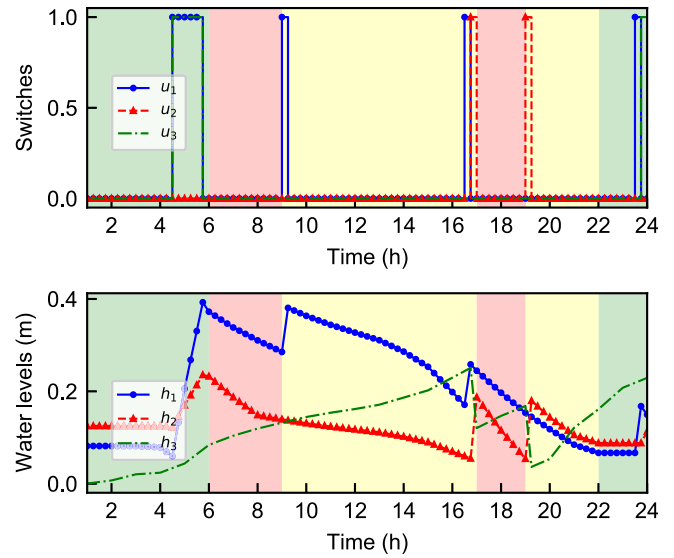


Fig. 8. Optimization results with  $p_s = 1$  and  $w_e = 100$

Table 3  
Cost of RWH-GWR components.

Item	Cost (R)
Rooftop PW tank	1473.39
Rooftop NPW tank	758.76
Underground tank	4235.80
Pumps	1240
Water treatment	8260
Contoller	10050
Accessories	6200
Installation	8200

Table 4  
Annual savings from the RWH-GWR system.

	Baseline	RWH-GWR	Savings
Potable water consumption			
Amount (m <sup>3</sup> )	501.88	359.70	28.33%
Cost (R)	12719.92	5538.40	56.46%
Wastewater discharged			
Amount (m <sup>3</sup> )	416.75	307.17	26.29%
Cost (R)	2894.76	1432.68	50.51%
Energy consumption			
Amount (kWh)	638.75	638.75	0.00%
Cost (R)	129.63	130.20	-0.43%
<b>Total operating cost (R)</b>	<b>15744.31</b>	<b>7101.28</b>	<b>54.90%</b>

Table 5  
Detailed economic analysis.

Year	Cash flow (R)	Discounted cash flow (R)	ADC (R)
0	-40417.95	-40417.95	-40417.95
1	10536.22	10015.42	-30402.53
2	10536.22	9520.36	-20882.17
3	10536.22	9049.77	-11832.40
4	10536.25	8602.47	-3229.94
5	10536.25	8177.25	4947.32

5.3. Energy water nexus

Fig. 8 is provided to demonstrate the ability of the modified objective function (36) in achieving different energy and water utilisation trade-off with the tuning factor  $w_e$  set to 100. It can be

seen from Fig. 8 that operation of the pumps are completely shifted out the peak demand periods in comparison to Fig. 6, resulting even more energy cost savings. In particular, the annual electricity cost with  $w_e = 100$  is reduced to 123.31 rand (4.88% decrease) and the annual potable water consumption in this case is increased to 384.59 m<sup>3</sup> (6.92% increase) in comparison to the optimization results given in Table 4.

5.4. Sensitivity analysis

Practically, there are uncertainties in the design parameters and there is a need to investigate the impact of these uncertainties on the performance of the proposed model. To this end, a sensitivity analysis of the important performance indicators of the proposed RWH-GWR system, namely, sizes of the three water tanks, capital cost, annual cost savings, and DPP of the project with respect to water demand, electricity price, discounting rate and rainfall intensity is performed. All of the four parameters are varied by factors of -20%, -10%, 10% and 20%, respectively, and the impacts on the performance indicators are determined and shown in Table 6. The sensitivity of the performance indicators is then calculated by (Ray et al., 2015)

$$s = \frac{dx/x}{dp/p} \tag{37}$$

where  $x$  and  $p$  represents the performance indicator and parameter, respectively. The sensitivity represents percentage changes in the performance indicators for 1% change in the design parameters. Calculation results are shown in Table 7. In Tables 6 and 7, the cells corresponding to a sensitivity value greater than 0.1 or less than -0.1 are highlighted for clarity.

Results in Tables 6 and 7 can be interpreted from two perspectives. From the design parameters' point of view, one can conclude that electricity price, discounting rate and rainfall intensity do not have much of an impact on the system's economic performance. Although they do affect the sizes of the water tanks, their impact on the capital cost, annual cost savings and DPP are quite limited. Comparatively speaking, the impacts of these three parameters have about the same magnitude. The most influential parameter is the water demand. Within [-20%, 20%] variation of the water

**Table 6**  
Sensitivity analysis results: percentage changes.

	T1 size	T2 size	T3 size	Capital cost	Annual cost savings	DPP
<b>water demand</b>						
20%	0.00%	10.92%	0.11%	0.16%	31.70%	-27.86%
10%	0.00%	5.30%	-3.14%	0.05%	14.27%	-14.82%
-10%	0.00%	-1.99%	-12.00%	-0.15%	-16.52%	25.07%
-20%	0.00%	6.04%	6.69%	0.16%	-39.13%	93.59%
<b>electricity price</b>						
20%	0.00%	10.09%	0.11%	0.15%	1.98%	-2.30%
10%	0.00%	16.15%	2.75%	0.27%	1.98%	-2.17%
-10%	0.00%	4.04%	13.30%	0.19%	1.98%	-2.25%
-20%	-3.11%	16.15%	0.11%	0.14%	1.97%	-2.30%
<b>discounting rate</b>						
20%	0.00%	16.15%	0.11%	0.24%	1.98%	0.71%
10%	0.00%	4.04%	13.30%	0.19%	1.98%	-0.82%
-10%	0.00%	4.04%	13.30%	0.19%	1.98%	-3.64%
-20%	0.00%	8.07%	1.45%	0.14%	1.98%	-5.06%
<b>rainfall intensity</b>						
20%	-0.22%	12.11%	22.56%	0.40%	1.99%	-2.04%
10%	0.00%	18.60%	9.36%	0.37%	1.98%	-2.05%
-10%	-3.61%	14.13%	-3.02%	0.06%	1.96%	-2.37%
-20%	0.00%	4.04%	1.85%	0.08%	1.93%	-2.32%

**Table 7**  
Sensitivity analysis results: sensitivity.

	T1 size	T2 size	T3 size	Capital cost	Annual cost savings	DPP
<b>water demand</b>						
20%	0.00	0.55	0.01	0.01	1.59	-1.39
10%	0.00	0.53	-0.31	0.00	1.43	-1.48
-10%	0.00	0.20	1.20	0.02	1.65	-2.51
-20%	0.00	-0.30	-0.33	-0.01	1.96	-4.68
<b>electricity price</b>						
20%	0.00	0.50	0.01	0.01	0.10	-0.12
10%	0.00	1.61	0.28	0.03	0.20	-0.22
-10%	0.00	-0.40	-1.33	-0.02	-0.20	0.22
-20%	0.16	-0.81	-0.01	-0.01	-0.10	0.11
<b>discounting rate</b>						
20%	0.00	0.81	0.01	0.01	0.10	0.04
10%	0.00	0.40	1.33	0.02	0.20	-0.08
-10%	0.00	-0.40	-1.33	-0.02	-0.20	0.36
-20%	0.00	-0.40	-0.07	-0.01	-0.10	0.25
<b>rainfall intensity</b>						
20%	-0.01	0.61	1.13	0.02	0.10	-0.10
10%	0.00	1.86	0.94	0.04	0.20	-0.21
-10%	0.36	-1.41	0.30	-0.01	-0.20	0.24
-20%	0.00	-0.20	-0.09	0.00	-0.10	0.12

demand, the capital cost of the project remains stable while the annual cost savings and DPP vary inversely with the water demand. When water demand goes up, the DPP will decrease and vice versa. To be exact, the DPP of the project decreases by more than 27% when the rainfall intensity is increased by 20% and the DPP is almost doubled when the rainfall intensity is reduced by 20%. This also agrees with published works, such as (Ghisi and de Oliveira, 2007), (Rahman et al., 2010), (Zhang et al., 2009), (Ghisi and Ferreira, 2007), that the RWH-GWR is economically more attractive for customers with high water demand. The water demand's impacts on the water tank sizes are similar to the other three parameters.

All parameters affect the sizes of the three tanks. Electricity price and rainfall intensity are the most influential parameters for the size of T2. The size of T3 is sensitive all the four parameters with no particular trend. Capital cost of the project is most robust against uncertainties in these parameters with negligible sensitivities values. Annual cost savings depends mostly on the water demand. Regarding the DPP, it is relatively stable for uncertainties in electricity price, discounting rate and rainfall intensity. It is affected noticeably by the water demand on the other hand. As mentioned

in the preceding paragraph, the proposed system is more beneficial for customers with high water demands. In particular, the DPP reduces to 3.17 years when the water demand increases by 20% while it shoots up to 8.15 years when the water demand falls by 20%. In all the other parameters' sensitivity analysis, the DPP ranges from 4.17 to 4.43 years.

## 6. Conclusion

A combined water tank sizing and pump operation optimization model is developed for integrated rainwater harvesting and grey-water recycling systems in residences. The model is validated by a case study in South Africa, a semi-arid country. Sensitivity analysis of the model results in terms of tank sizes, annual cost savings and the discounted payback period of the proposed solution with respect to design four parameters is performed. The results show that the model is most sensitive to the end-user water demand and the least sensitive to the electricity price increase.  $\pm 20\%$  change in discounting rate and rainfall intensity also have a limited impact on the system's performance. The project capital cost and annual cost savings remain stable irrespective of all of the four design

parameters investigated. Overall, the proposed system results in an economically attractive solution for residential users with more than 50% annual cost savings and a discounted payback period of about 5 years. The findings of the study indicate that when combined, greywater recycling and rainwater harvesting could provide a beneficial residential water supply solution with acceptable economic performance. Local governments and municipalities should consider to provide rebates and incentives to such projects. This will reduce the investment cost and improve the financial attractiveness of such projects for a wider adoption, which will promote sustainable utilisation of the scarce water resource. Future research directions include integration of renewable energy sour-

$$b_1 = \begin{bmatrix} -h_1(0) + \frac{1}{A_{t1}}D_{pw}(1) \\ -h_1(0) + \frac{1}{A_{t1}}[D_{pw}(1) + D_{pw}(2)] \\ \vdots \\ -h_1(0) + \frac{1}{A_{t1}}[D_{pw}(1) + \dots + D_{pw}(N)] \end{bmatrix}_{N \times 1}, \tag{39}$$

$$M_2 = -\frac{t_s}{A_{t1}} \begin{bmatrix} 0 & 0 & 0 & Q_1 & 0 & \dots & 0 & 0 & \dots & 0 & -Q_3 & 0 & \dots & 0 & 0 & \dots & 0 & 0 & \dots & 0 \\ 0 & 0 & 0 & Q_1 & Q_1 & \dots & 0 & 0 & \dots & 0 & -Q_3 & -Q_3 & \dots & 0 & 0 & \dots & 0 & 0 & \dots & 0 \\ \vdots & \vdots & \vdots & \vdots & \vdots & \ddots & \vdots & \vdots & \ddots & \vdots & \vdots & \vdots & \ddots & \vdots & \vdots & \ddots & \vdots & \vdots & \ddots & \vdots \\ 0 & 0 & 0 & Q_1 & Q_1 & \dots & Q_1 & 0 & \dots & 0 & -Q_3 & -Q_3 & \dots & -Q_3 & 0 & \dots & 0 & 0 & \dots & 0 \end{bmatrix}_{N \times (3+5N)}, \tag{40}$$

ces to support the water supply system, integrated operation scheduling of the water supply system and home appliances, and investigation of the applicability of the proposed system in different climate zones.

**Declaration of competing interest**

The authors declare that they have no known competing financial interests or personal relationships that could have appeared to influence the work reported in this paper.

$$b_2 = \begin{bmatrix} h_1(0) - h_1^{min} - \frac{1}{A_{t1}}D_{pw}(1) \\ h_1(0) - h_1^{min} - \frac{1}{A_{t1}}[D_{pw}(1) + D_{pw}(2)] \\ \vdots \\ h_1(0) - h_1^{min} - \frac{1}{A_{t1}}[D_{pw}(1) + \dots + D_{pw}(N)] \end{bmatrix}_{N \times 1}, \tag{41}$$

$$M_3 = \frac{t_s}{A_{t2}} \begin{bmatrix} 0 & -1 & 0 & 0 & \dots & 0 & Q_2 & 0 & \dots & 0 & Q_3 & 0 & \dots & 0 & 0 & \dots & 0 & 0 & \dots & 0 \\ 0 & -1 & 0 & 0 & \dots & 0 & Q_2 & Q_2 & \dots & 0 & Q_3 & Q_3 & \dots & 0 & 0 & \dots & 0 & 0 & \dots & 0 \\ \vdots & \vdots & \vdots & \vdots & \ddots & \vdots & \vdots & \vdots & \ddots & \vdots & \vdots & \vdots & \ddots & \vdots & \vdots & \ddots & \vdots & \vdots & \ddots & \vdots \\ 0 & -1 & 0 & 0 & \dots & 0 & Q_2 & Q_2 & \dots & Q_2 & Q_3 & Q_3 & \dots & Q_3 & 0 & \dots & 0 & 0 & \dots & 0 \end{bmatrix}_{N \times (3+5N)}, \tag{42}$$

**Acknowledgements**

Ambrose Njepu would like to thank the MasterCard Foundation Scholarship Program (MCFSP) for providing financial support to his study.

**Appendix. Appendix**

The elements of the constraint matrices and vectors in (26) are given here. In particular,  $M_1, M_2, M_3, M_4, M_5$  and  $M_6$  are matrices of the inequality constraints (19), (20) and (21), while  $b_1, b_2, b_3, b_4, b_5$  and  $b_6$  are the corresponding vectors.  $M_7$  and  $b_7$  are the matrix and vector of the auxiliary variables in (15), (16), (17) and (18).

$$b_3 = \begin{bmatrix} -h_2(0) + \frac{1}{A_{t2}}D_{npw}(1) \\ -h_2(0) + \frac{1}{A_{t2}}[D_{npw}(1) + D_{npw}(2)] \\ \vdots \\ -h_2(0) + \frac{1}{A_{t2}}[D_{npw}(1) + \dots + D_{npw}(N)] \end{bmatrix}_{N \times 1}, \tag{43}$$

$$M_1 = \frac{t_s}{A_{t1}} \begin{bmatrix} -1 & 0 & 0 & Q_1 & 0 & \dots & 0 & 0 & \dots & 0 & -Q_3 & 0 & \dots & 0 & 0 & \dots & 0 & 0 & \dots & 0 \\ -1 & 0 & 0 & Q_1 & Q_1 & \dots & 0 & 0 & \dots & 0 & -Q_3 & -Q_3 & \dots & 0 & 0 & \dots & 0 & 0 & \dots & 0 \\ \vdots & \vdots & \vdots & \vdots & \vdots & \ddots & \vdots & \vdots & \ddots & \vdots & \vdots & \vdots & \ddots & \vdots & \vdots & \ddots & \vdots & \vdots & \ddots & \vdots \\ -1 & 0 & 0 & Q_1 & Q_1 & \dots & Q_1 & 0 & \dots & 0 & -Q_3 & -Q_3 & \dots & -Q_3 & 0 & \dots & 0 & 0 & \dots & 0 \end{bmatrix}_{N \times (3+5N)}, \tag{38}$$

$$M_4 = -\frac{t_s}{A_{t2}} \begin{bmatrix} 0 & 0 & 0 & 0 & \dots & 0 & Q_2 & 0 & \dots & 0 & Q_3 & 0 & \dots & 0 & 0 & \dots & 0 & 0 & \dots & 0 \\ 0 & 0 & 0 & 0 & \dots & 0 & Q_2 & Q_2 & \dots & 0 & Q_3 & Q_3 & \dots & 0 & 0 & \dots & 0 & 0 & \dots & 0 \\ \vdots & \vdots & \vdots & \vdots & \ddots & \vdots & \vdots & \vdots & \ddots & \vdots & \vdots & \vdots & \ddots & \vdots & \vdots & \ddots & \vdots & \vdots & \ddots & \vdots \\ 0 & 0 & 0 & 0 & \dots & 0 & Q_2 & Q_2 & \dots & Q_2 & Q_3 & Q_3 & \dots & Q_3 & 0 & \dots & 0 & 0 & \dots & 0 \end{bmatrix}_{N \times (3+5N)}, \tag{44}$$

$$b_4 = \begin{bmatrix} h_2(0) - h_2^{min} - \frac{1}{A_{t2}} D_{npw}(1) \\ h_2(0) - h_2^{min} - \frac{1}{A_{t2}} [D_{npw}(1) + D_{npw}(2)] \\ \vdots \\ h_2(0) - h_2^{min} - \frac{1}{A_{t2}} [D_{npw}(1) + \dots + D_{npw}(N)] \end{bmatrix}_{N \times 1}, \tag{45}$$

$$M_5 = \frac{t_s}{A_{t3}} \begin{bmatrix} 0 & 0 & -1 & 0 & \dots & 0 & -Q_2 & 0 & \dots & 0 & 0 & \dots & 0 & 0 & \dots & 0 & 0 & \dots & 0 \\ 0 & 0 & -1 & 0 & \dots & 0 & -Q_2 & -Q_2 & \dots & 0 & 0 & \dots & 0 & 0 & \dots & 0 & 0 & \dots & 0 \\ \vdots & \vdots & \vdots & \vdots & \ddots & \vdots & \vdots & \vdots & \ddots & \vdots & \vdots & \ddots & \vdots & \vdots & \ddots & \vdots & \vdots & \ddots & \vdots \\ 0 & 0 & -1 & 0 & \dots & 0 & -Q_2 & -Q_2 & \dots & -Q_2 & 0 & \dots & 0 & 0 & \dots & 0 & 0 & \dots & 0 \end{bmatrix}_{N \times (3+5N)}, \tag{46}$$

$$b_5 = \begin{bmatrix} -h_3(0) - \frac{1}{A_{t3}} [V_{gw}(1) + V_{rw}(1) - V_{ov}(1)] \\ -h_3(0) - \frac{1}{A_{t3}} [(V_{gw}(1) + V_{gw}(2)) + (V_{rw}(1) + V_{rw}(2)) - (V_{ov}(1) + V_{ov}(2))] \\ \vdots \\ -h_3(0) - \frac{1}{A_{t3}} [(V_{gw}(1) + \dots + V_{gw}(N)) + (V_{rw}(1) + \dots + V_{rw}(N)) - (V_{ov}(1) + \dots + V_{ov}(N))] \end{bmatrix}_{N \times 1}, \tag{47}$$

$$M_6 = \frac{t_s}{A_{t3}} \begin{bmatrix} 0 & 0 & 0 & 0 & \dots & 0 & Q_2 & 0 & \dots & 0 & 0 & \dots & 0 & 0 & \dots & 0 & 0 & \dots & 0 \\ 0 & 0 & 0 & 0 & \dots & 0 & Q_2 & Q_2 & \dots & 0 & 0 & \dots & 0 & 0 & \dots & 0 & 0 & \dots & 0 \\ \vdots & \vdots & \vdots & \vdots & \ddots & \vdots & \vdots & \vdots & \ddots & \vdots & \vdots & \ddots & \vdots & \vdots & \ddots & \vdots & \vdots & \ddots & \vdots \\ 0 & 0 & 0 & 0 & \dots & 0 & Q_2 & Q_2 & \dots & Q_2 & 0 & \dots & 0 & 0 & \dots & 0 & 0 & \dots & 0 \end{bmatrix}_{N \times (3+5N)}, \tag{48}$$

$$b_6 = \begin{bmatrix} h_3(0) - h_3^{min} + \frac{1}{A_{t3}} [V_{gw}(1) + V_{rw}(1) - V_{ov}(1)] \\ h_3(0) - h_3^{min} + \frac{1}{A_{t3}} [(V_{gw}(1) + V_{gw}(2)) + (V_{rw}(1) + V_{rw}(2)) - (V_{ov}(1) + V_{ov}(2))] \\ \vdots \\ h_3(0) - h_3^{min} + \frac{1}{A_{t3}} [(V_{gw}(1) + \dots + V_{gw}(N)) + (V_{rw}(1) + \dots + V_{rw}(N)) - (V_{ov}(1) + \dots + V_{ov}(N))] \end{bmatrix}_{N \times 1}, \tag{49}$$

$$M_7 = t_s \begin{bmatrix} 0 & 0 & 0 & 1 & 0 & \dots & 0 & 0 & 1 & 0 & \dots & 0 & 0 & 0 & \dots & 0 & -1 & 0 & \dots & 0 & -1 & 0 & \dots & 0 \\ 0 & 0 & 0 & -1 & 1 & \dots & 0 & 0 & -1 & 1 & \dots & 0 & 0 & 0 & \dots & 0 & 0 & -1 & \dots & 0 & 0 & -1 & \dots & 0 \\ \vdots & \vdots & \vdots & \vdots & \vdots & \ddots & \vdots & \vdots & \vdots & \vdots & \ddots & \vdots & \vdots & \ddots & \vdots & \vdots & \vdots & \ddots & \vdots & \vdots & \vdots & \ddots & \vdots \\ 0 & 0 & 0 & 0 & 0 & \dots & -1 & 1 & 0 & 0 & \dots & -1 & 1 & 0 & \dots & 0 & 0 & \dots & -1 & 0 & 0 & \dots & -1 \end{bmatrix}_{N \times (3+5N)}, \tag{50}$$

$$b_7 = [0 \quad \dots \quad 0]_{N \times 1}^T, \tag{51}$$



## References

- Al-Jayyousi, O.R., 2003. Greywater reuse: towards sustainable water management. *Desalination* 156, 181–192.
- Boers, T.M., Ben-Asher, J., 1982. A review of rainwater harvesting. *Agric. Water Manag.* 5, 145–158.
- Boyjoo, Y., Pareek, V.K., Ang, M., 2013. A review of greywater characteristics and treatment processes. *Water Sci. Technol.* 67, 1403–1424.
- Campisano, A., Modica, C., 2012. Optimal sizing of storage tanks for domestic rainwater harvesting in Sicily. *Resour. Conserv. Recycl.* 63, 9–16.
- Chilton, J.C., Maidment, G.G., Marriott, D., Francis, A., Tobias, G., 2000. Case study of a rainwater recovery system in a commercial building with a large roof. *Urban Water* 1, 345–354.
- Christova-Boal, D., Eden, R.E., McFarlane, S., 1996. An investigation into greywater reuse for urban residential properties. *Desalination* 106, 391–397.
- Council, N.I., 2013. *Global Trends 2030: Alternative Worlds*. Central Intelligence Agency.
- Cureau, R.J., Ghisi, E., 2020. Electricity savings by reducing water consumption in a whole city: a case study in Joinville, southern Brazil. *J. Clean. Prod.* 261, 121194.
- Domènech, L., Saurí, D., 2011. A comparative appraisal of the use of rainwater harvesting in single and multi-family buildings of the metropolitan area of Barcelona (Spain): social experience, drinking water savings and economic costs. *J. Clean. Prod.* 19, 598–608.
- Farreny, R., Morales-Pinzón, T., Guisasaola, A., Taya, C., Rieradevall, J., Gabarrell, X., 2011. Roof selection for rainwater harvesting: quantity and quality assessments in Spain. *Water Res.* 45, 3245–3254.
- Ghisi, E., Bressan, D.L., Martini, M., 2007. Rainwater tank capacity and potential for potable water savings by using rainwater in the residential sector of south-eastern Brazil. *Build. Environ.* 42, 1654–1666.
- Ghisi, E., Ferreira, D.F., 2007. Potential for potable water savings by using rainwater and greywater in a multi-storey residential building in southern Brazil. *Build. Environ.* 42, 2512–2522.
- Ghisi, E., de Oliveira, S.M., 2007. Potential for potable water savings by combining the use of rainwater and greywater in houses in southern Brazil. *Build. Environ.* 42, 1731–1742.
- Ghisi, E., Schondermark, P.N., 2013. Investment feasibility analysis of rainwater use in residences. *Water Resour. Manag.* 27, 2555–2576.
- Ghunmi, L.A., Zeeman, G., Fayyad, M., Van Lier, J.B., 2011. Grey water treatment systems: a review. *Environ. Sci. Technol.* 41, 657–698.
- Gleeson, T., VanderSteen, J., Sophocleous, M.A., Taniguchi, M., Alley, W.M., Allen, D.M., Zhou, Y., 2010. Groundwater sustainability strategies. *Nat. Geosci.* 3, 378.
- Gwenzi, W., Dunjana, N., Pisa, C., Tauro, T., Nyamadzawo, G., 2015. Water quality and public health risks associated with roof rainwater harvesting systems for potable supply: review and perspectives. *Sustain. Water Qual. Ecol.* 6, 107–118.
- Huang, Z., Fang, B., Deng, J., 2020. Multi-objective optimization strategy for distribution network considering v2g-enabled electric vehicles in building integrated energy system. *Prot. Control Mod. Power Syst.* 5.
- Ilemobade, A.A., Olanrewaju, O.O., Griffioen, M.L., 2013. Greywater reuse for toilet flushing at a university academic and residential building. *Water South Africa* 39, 351–360.
- Imteaz, M.A., Shanableh, A., Rahman, A., Ahsan, A., 2011. Optimisation of rainwater tank design from large roofs: a case study in Melbourne, Australia. *Resour. Conserv. Recycl.* 55, 1022–1029.
- Jacobsen, M., Webster, M., Vairavamoorthy, K., 2012. The future of water in African cities: why waste water? World Bank.
- Jeong, H., Broesicke, O.A., Drew, B., Crittenden, J.C., 2018. Life cycle assessment of small-scale greywater reclamation systems combined with conventional centralized water systems for the City of Atlanta, Georgia. *J. Clean. Prod.* 174, 333–342.
- Karim, M.R., Rimi, R.A., Billah, M.S., 2013. Reliability analysis of household rainwater harvesting tanks in the coastal areas of Bangladesh using daily water balance model. *20th Int. Congr. Model. Simul.* 2639–2645.
- Khastagir, A., Jayasuriya, N., 2010. Optimal sizing of rain water tanks for domestic water conservation. *J. Hydrol.* 381, 181–188.
- Kim, R.H., Lee, S., Jeong, J., Lee, J.H., Kim, Y.K., 2007. Reuse of greywater and rainwater using fiber filter media and metal membrane. *Desalination* 202, 326–332.
- Komeh, Z., Memarian, H., Tajbakhsh, S.M., 2017. Reservoir volume optimization and performance evaluation of rooftop catchment systems in arid regions: a case study of Birjand, Iran. *Water Sci. Eng.* 10, 125–133.
- Lansley, K.E., Awumah, K., 1994. Optimal pump operations considering pump switches. *J. Water Resour. Plann. Manag.* 120, 17–35.
- Leong, J.Y.C., Chong, M.N., Poh, P.E., 2018. Assessment of greywater quality and performance of a pilot-scale decentralised hybrid rainwater-greywater system. *J. Clean. Prod.* 172, 81–91.
- Letsoalo, A., Blignaut, J., De Wit, T., De Wit, M., Hess, S., Tol, R.S.J., Van Heerden, J., 2007. Triple dividends of water consumption charges in South Africa. *Water Resour. Res.* 43.
- Li, F., Wichmann, K., Otterpohl, R., 2009. Review of the technological approaches for grey water treatment and reuses. *Sci. Total Environ.* 407, 3439–3449.
- Mathaba, T., Xia, X., Zhang, J., 2014. Analysing the economic benefit of electricity price forecast in industrial load scheduling. *Elec. Power Syst. Res.* 116, 158–165.
- Matos, C., Santos, C., Pereira, S., Bentes, I., Imteaz, M., 2013. Rainwater storage tank sizing: case study of a commercial building. *Int. J. Sustain. Built Environ.* 2, 109–118.
- Menke, R., Abraham, E., Parpas, P., Stoianov, I., 2016. Demonstrating demand response from water distribution system through pump scheduling. *Appl. Energy* 170, 377–387.
- Notaro, V., Liuzzo, L., Freni, G., 2016. Reliability analysis of rainwater harvesting systems in southern Italy. *Procedia Eng* 162, 373–380.
- Okoye, C.O., Solyali, O., Akintug, B., 2015. Optimal sizing of storage tanks in domestic rainwater harvesting systems: a linear programming approach. *Resour. Conserv. Recycl.* 104, 131–140.
- Organization, W.H., 2006. *Guidelines for the Safe Use of Wastewater, Excreta and Greywater*, ume 1. World Health Organization.
- Pinto, F.S., Marques, R.C., 2017. Desalination projects economic feasibility: a standardization of cost determinants. *Renew. Sustain. Energy Rev.* 78, 904–915.
- Prathapar, S.A., Jamrah, A., Ahmed, M., Al Adawi, S., Al Sidairi, S., Al Harassi, A., 2005. Overcoming constraints in treated greywater reuse in Oman. *Desalination* 186, 177–186.
- Rahman, A., Dbais, J., Imteaz, M.A., 2010. Sustainability of rainwater harvesting systems in multistorey residential buildings. *Am. J. Eng. Appl. Sci.* 3, 73–82.
- Ray, S., Mukherjee, J., Mandal, S., 2015. Chapter 13 - modelling nitrogen and carbon cycles in hooghly estuary along with adjacent mangrove ecosystem. In: Park, Y.S., Lek, S., Baehr, C., Jørgensen, S.E. (Eds.), *Adv. Model. Tech. Stud. Glob. Chang. Environ. Sci.* Elsevier. Volume 27 of *Developments In Environmental Modelling*, pp. 289–320.
- Sanchez, A.S., Cohim, E., Kalid, R.A., 2015. A review on physicochemical and microbiological contamination of roof-harvested rainwater in urban areas. *Sustain. Water Qual. Ecol.* 6, 119–137.
- Sasmita, M., 2010. *Engineering Economics and Costing*, second ed. PHI Learning Pvt. Ltd, New Delhi.
- Siang, K.O., Leong, J.Y.C., Poh, P.E., Chong Meng Nan, E.V.L., 2018. A review of greywater recycling related issues: challenges and future prospects in Malaysia. *J. Clean. Prod.* 171, 17–29.
- Soares Gerdali, M., Ghisi, E., 2018. Assessment of the length of rainfall time series for rainwater harvesting in buildings. *Resour. Conserv. Recycl.* 133, 231–241.
- Su, M.D., Lin, C.H., Chang, L.F., Kang, J.L., Lin, M.C., 2009. A probabilistic approach to rainwater harvesting systems design and evaluation. *Resour. Conserv. Recycl.* 53, 393–399.
- Thapa, B.R., Ishidaira, H., Pandey, V.P., Shakya, N.M., 2017. A multi-model approach for analyzing water balance dynamics in Kathmandu Valley, Nepal. *J. Hydrol. Reg. Stud.* 9, 149–162.
- UNDP, 2015. *Sustainable development goals*. Technical Report.
- UNESCO, 2003. *The united nations world water development report*. UNESCO.
- Vörösmarty, C.J., Green, P., Salisbury, J., Lammers, R.B., 2000. Global water resources: vulnerability from climate change and population growth. *Science* 289, 284–288.
- Wanjiru, E., Xia, X., 2018. Sustainable energy-water management for residential houses with optimal integrated grey and rain water recycling. *J. Clean. Prod.* 170, 1151–1166.
- Zhang, D., Gersberg, R.M., Wilhelm, C., Voigt, M., 2009. Decentralized water management: rainwater harvesting and greywater reuse in an urban area of Beijing, China. *Urban Water J.* 6, 375–385.
- Zhuan, X., Xia, X., 2013. Optimal operation scheduling of a pumping station with multiple pumps. *Appl. Energy* 104, 250–257.
- van Zyl, J.E., Savic, D.A., Walters, G.A., 2004. Operational optimization of water distribution systems using a hybrid genetic algorithm. *J. Water Resour. Plann. Manag.* 130, 160–170.